Journal of Magnetic Resonance 306 (2019) 167–172

Contents lists available at ScienceDirect

Journal of Magnetic Resonance

journal homepage: www.elsevier.com/locate/jmr

H-MAS

Ago Samoson

Tallinn University of Technology, Estonia

ARTICLE INFO

Article history:
Received 15 May 2019
Revised 26 June 2019
Accepted 8 July 2019
Available online 11 July 2019

Keyword:
MAS
Structural biology

ABSTRACT

We characterize a new generation of MAS probes, designed for 1H detection in solid and viscous structures. High top speed (currently 170 kHz), existence of a wide speed range and quick acceleration enable numerous new experiment categories. Most notably, massive biomolecular structures become amenable to a detailed structural and dynamics studies.

Over the last twenty years the development of ever faster MAS has enabled spectacular improvements for resolution and sensitivity in biomolecular solid-state NMR, allowing detailed structural and dynamics studies of increasing complexity. Numerous novel possibilities and experiment categories, all induced by the resolved H resonances and technical virtues of sub-mm rotors, are illustrated here with the characterisation of a new generation of MAS probes, designed for ^{1}H detection in solid and viscous structures, and capable of >170 kHz top speeds.

A prevailing volume of NMR work indicates that there must be some good reason for ^{1}H detection. Informative chemical shift range, high sensitivity and absolute natural abundance have earned hydrogen atoms a solid position in the biochemical and -medical research by solution NMR. In solid and viscous structures, however, the practice has been very different. An embarrassing, half a century long lack of practical methods to resolve ^{1}H positions by the chemical shift has limited options to ^{13}C MAS and a relatively limited number of "comfortable" molecules amenable to a sensible study. As a result, only very few high-field spectrometers are accessible to MAS, most are kept busy with "high resolution" study of solvated structures.

The situation started to change in 2012 with the first announcement of 100 kHz MAS at EUROMAR in Dublin [1]. Since then, elevated MAS speeds have allowed to do protein structures principally from scratch [2], determine a docking of sizable molecular complexes [3] and introduce a direct way to track dynamics. Numerous applications have been escorted by a gradual increase in the spinning rates to 126 [4] and 140 kHz [5].

Although the design, materials and machining present considerable challenges for keeping required nanometric tolerances, the principal limit to top speed is set by the strength of rotor wall material. Metastable zirconium oxide is currently a material of choice, providing a working compromise of the processing effort and mechanical reliability. This leaves a reduction of the diameter as a first technical solution to increase the speeds any further. We have developed series of fast spinning systems, optimized for the speed ⊗ volume product. With the rotors of ca 0.5 mm in diameter we have reached the rates over 170 kHz (Fig. 1).

Extrapolation to an infinite drive pressure would decrease the rotation period to 4.66 μs, which amounts to 225 kHz and 344 m/s rotor surface speed, equal to the speed of sound in air. Obviously, the drive efficiency is one of the technical hurdles in achieving higher spinning rates and preserving still any reasonable amount of the sample. The reduction of rotor diameter (D) decreases the sensitivity in principle quadratically as $1/D^2$ [6]. However, turns out that the higher γ_H and better filling factor due to a more concentrated sample will actually compensate for the reduced volume. The fastest rotors pack currently about 200 nL sample. Assuming ca 30% water to ensure native flexibility and resolution, ca 0.12 mg of a protein will be then measured. For a comparison, in solutions the sample coil volume is 1000× larger (D = 5.0 mm) and the whole required solution volume twice of that, extending below and above the measurement section. As the efficiency of a saddle coil is about half of the solenoid, a factor of two more sample would be required for the same principal efficiency. The magic instead of 90° angle penalizes MAS by factor of sin(54.7°) = 0.82. Considering these multipliers, H-MAS geometry and filling factor scale up to a measurement of 0.12 * 1000 * 2 * 2 * 0.82 = 400 mg protein in a solution tube. Since the "rotor" diameter of the solution sample tube is 10× larger, the sensitivity scales up by 10^2 times and respectively less sample is actually required, 400/100 = 4 mg, to get the

https://doi.org/10.1016/j.jmr.2019.07.010
1090-7807/

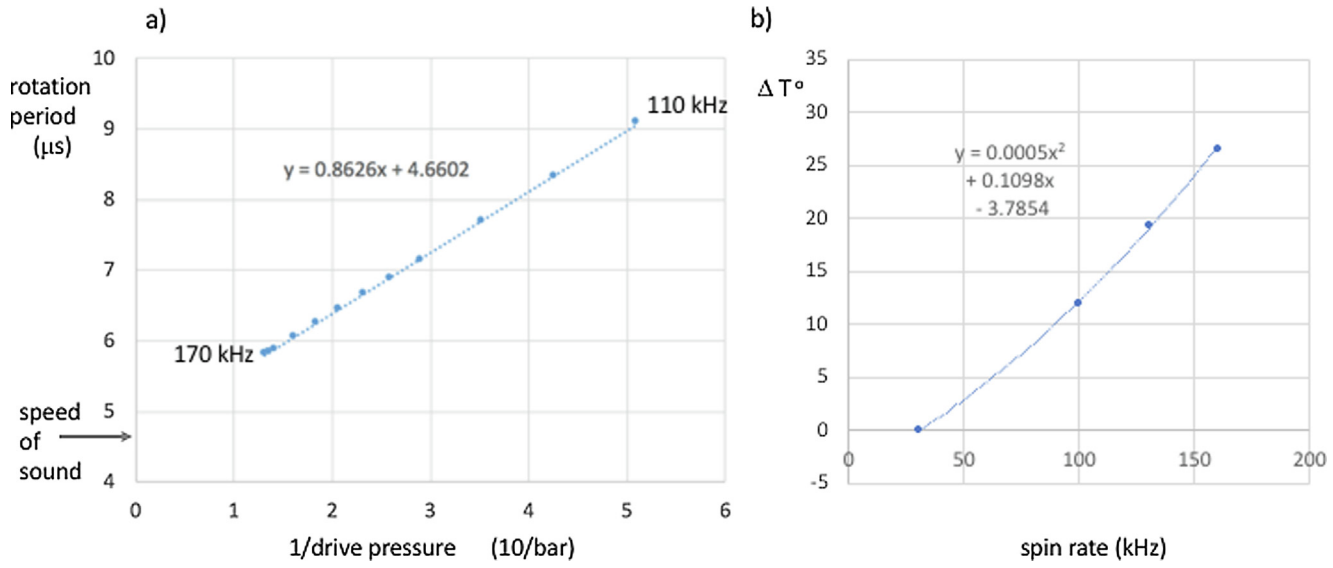

Fig. 1. (a) Rotation period dependency on drive gas (air) pressure (inverse scale). (b) Temperature rise with the spinning rate.

same sensitivity as with the small MAS coil optimized for a 0.5 mm rotor. Practically, for a typical 0.1 mM concentration, about 5 mg of 20 kDa protein is used in order to get ^{1}H lines resolved to 20 Hz without having to rely on a deuteration. It appears from these considerations/conditions that the H-MAS integral sensitivity is technically very comparable to the solution S/N. This conclusion is a subject to two practical corrections: linewidth and T_1 relaxation differences. They may nearly cancel each other out, if paramagnetic relaxation agents are used in high speed MAS [7]. However, a considerable ≈50× difference remains in the required amount of the sample and isotopes. The difference may be even more of a game changer in transition from ^{13}C-MAS to ^{1}H-MAS [8]. For an optimal resolution, a preparation of (nano) crystals may be also needed which can be a very demanding process. Transition from D = 2–4 mm rotors to 0.5 means respectively 16–64 times less signal, which is compensated by a product of polarization, magnetic moment and induction as $(\gamma_H/\gamma_C)^3 = 63$. The white noise voltage grows with frequency by $\sqrt{4}$, but this noise increase compensated by a $\sqrt{4}$ bandwidth factor, considering about four times reduced ^{1}H spectral span, 15 ppm against 250 ppm of ^{13}C. All things considered, the transition to ^{1}H detection from fully enriched ^{13}C in organic solids does not reduce S/N if a similar linewidth is achieved. Moreover, J-coupling based polarization transfers can be about 1.4 times (observed experimentally by S. Penzel) more efficient than Hartman-Hahn CP. It is also pertinent to note that the effective CP-active sample volume, where the rotation frequency offset makes B_1 field profiles match the CP condition, reduces with the increasing rotation rate (explained graphically in Fig. 2a). This and possibly also suppressed spin diffusion within a thermal "spin bath" at higher rotation rate lead to significant loss of CP efficiency in it's basic form (Fig. 2b).

The INEPT polarization transfer advantage can be compounded by ca 1.5 times higher hydrogen content compared to carbon in a typical protein structure. ^{1}H detection, as preferred and dominantly used in a solution ecosystem, carries also more quality in spectral information, and the required sample(isotope) amount is reduced by $(4/0.5)^3 * 1.4 * 1.5 \approx 1000\times$ compared to ^{13}C MAS. Quite intriguing is also a possibility to investigate the samples in a form of a small single crystal [9] instead of powder collection.

Handling of sub-mm rotors requires special tools and vision enhancement. Axial rotor symmetry and filling quality can be critical to the performance and stability at higher spinning rates. A good indicative of this is a smoothness of passing mechanical resonances. At those points, a whirling motion will get amplified, in worst case to the extent of preventing any speed increase, Fig. 3.

The availability of an extended spinning range allows a measurement of the homogeneous contribution to linewidth directly as an alternative to the spin-echo sequence. However, a certain care should be taken to eliminate the temperature effect on mobile structures. The spinning at 170 kHz equals to 80% sound speed at the rotor surface, generating a frictional heating by Δ44° above room temperature in quadratic extrapolation. Flushing the coil compartment by just 3–4 L/min by 5 °C output from a vortex cooler reduces the sample temperature over Δ20° centigrade. A hexamethylbenzene (HMB) ^{1}H linewidth dependency on rotation period shows a slight quadratic component in both cooled and not cooled cases (Fig. 4).

Introduction of a speed dependent correction straightens the linewidth plot to linear within an experimental error and allows to determine, also extrapolate the homogeneous linebroadening to yet higher speeds. This assumption is corroborated by a similar linear dependency observed in a diluted protein spin system (back-deuterated ubiqutin) and on ^{23}NaCl, where the dipolar interactions are scaled down even further by the virtue of lower γ_{Na}. On median a much sharper dependency is observed in a dipeptide Asp-Ala [10], which is a representative of relatively rigid (with the exception of methyl and amide groups) strongly coupled spin system in an organic structure. The difference seems to be quantitative compared to, in the average 4.6 times lower, proton spin density in a proton diluted system. A similar regularity was reported in adamantine [11]. Interestingly, median linewidth of fully protonated ubiquitin exhibits even sharper rotation period dependency, this is presumably an effect of structural dynamics which spoils the spin phase refocussing over rotation period. Although the mobility is not affected by spin dilution, its effect is relatively weaker from a distant spin and thus perdeuterated/diluted ubiquitin resembles more of a rigid structure. Dynamics may also contribute to observed quadratic speed dependencies. The motions much faster than rotation are represented by adamantane and hexamethylbenzene, where effective spin distances measure from the center of molecular motion and broadening coefficient is intermediate. The extrapolations to higher speeds do not predict the resolution as such, since in solid and viscous systems shape effects, crystal packing, bond dispersions, J-couplings, mobility and

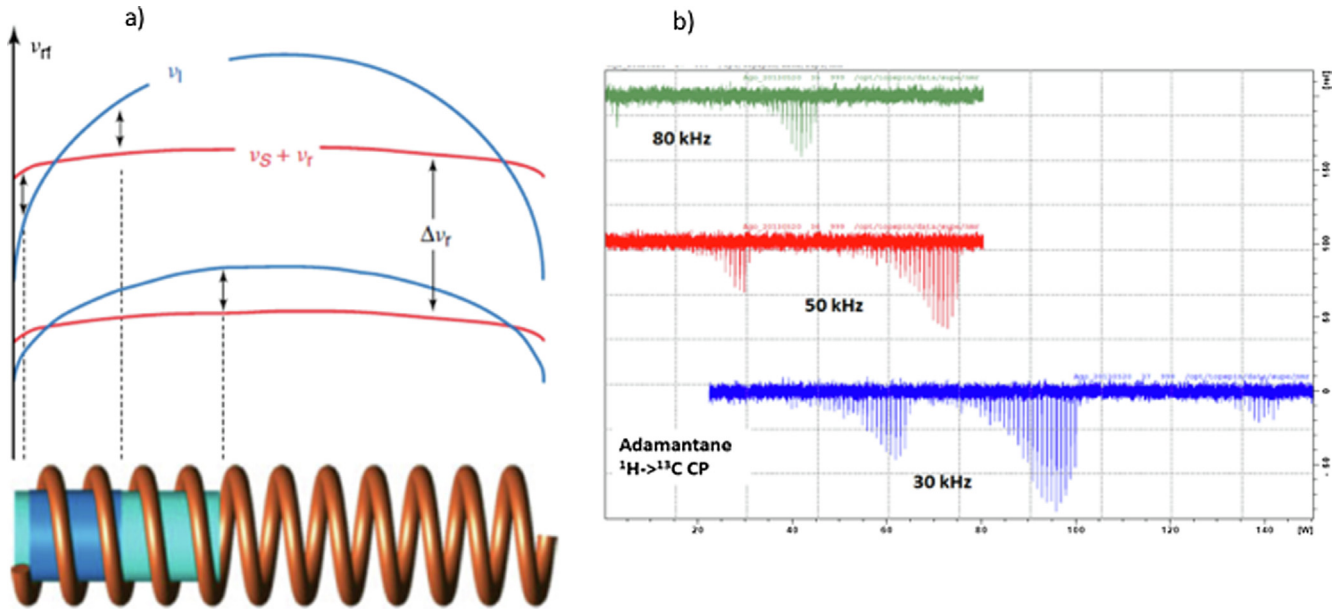

Fig. 2. (a) CP matching at fast spinning rate. *rf* amplitude at the end of (long) solenoid drops principally to half of its center value. A uniform profile displacement of one B_1 field leaves only a small part (blue) of sample (cyan, shown partially) active for the CP process. The active fraction is reduced with increasing rotation rate ν_r. (b) CP Hartman-Hahn mismatch experiment series on adamantane at three rotation rates. CP signal drops drastically with the increasing rotation rate. (For interpretation of the references to colour in this figure legend, the reader is referred to the web version of this article.)

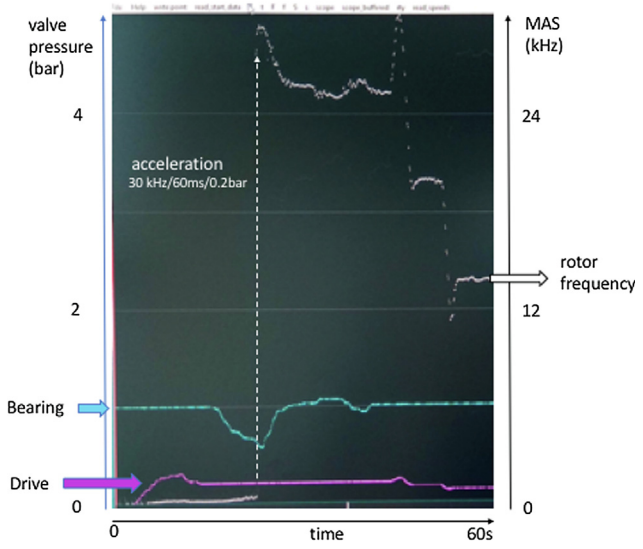

Fig. 3. MAS spectrogram, showing a time-flow of applied pressures and rotation rate. Initially the speed does not increase despite adding the drive pressure, since all the energy goes in a mechanical vibration at an eigenfrequency of the rotor/gas-buffer/housing system, effectively a harmonic oscillator. Reduction of the force constant (bearing pressure) allows to "tunnel" the spinning through a barrier of the mechanical resonances.

perhaps some more factors may contribute to the line broadening. However, from presented data we can say that protein MAS homogeneous broadening at the rotor period of 6 μs (6 * 12 = 72 Hz) does not contribute more than about 0.06 ppm at highest, 1.2 GHz fields as announced recently. This linebroadening does not suffer from a size of biomolecular structure or increase of the magnetic field like in solvents, on the contrary, increased spectral span may help to suppress the residual spin-flips.

A mechanistic comparison of the line-broadening origin in two different ecosystems can be conjectured as a random walk concept. Thermal fast motion limit, a basis of solvent line narrowing, can be generally understood as a random spin coherence dephasing. Accumulation of single instance phase increments

$$2\pi\phi \cdot \tau$$

after T/τ random walk steps leads to a statistical dephasing

$$\Phi = 2\pi\phi \cdot \tau\sqrt{\frac{T}{\tau}}$$

where τ is a characteristic correlation time for an interaction ϕ, which itself assumes random nonperiodic values of varying sign. Due to the shortness of correlation time τ, a phase of $\Phi = 2\pi$, may take seconds to accumulate

$$T_2' = \frac{1}{\tau\phi^2}$$

While in solutions the interaction value and step direction change fast and randomly, the MAS, on the contrary, renders interactions periodical, principally proportional to

$$\phi = -A\cos(\omega t)[-A_2\cos(2\omega t) + B\sin(\omega t) + B_2\sin(2\omega t)$$

where *A,B* represent all orientational and tensorial functions (we shall omit details and expression in square brackets for a convenience) and $\omega = 2\pi\nu_r$. Whereas the interaction strength remains about the same as in solution, the correlation time associated with rotation is many orders longer from solvent thermal correlations, yet the line broadenings we observe at high MAS speeds are not so different from liquids. In order to understand and compare two mechanisms of the spectral enhancement, we hypothesize that in MAS conditions the correlation time can be considered as a gap between random spin-flips. The integration over τ gives for the phase increment instance a value which is inversely proportional to the rotation speed

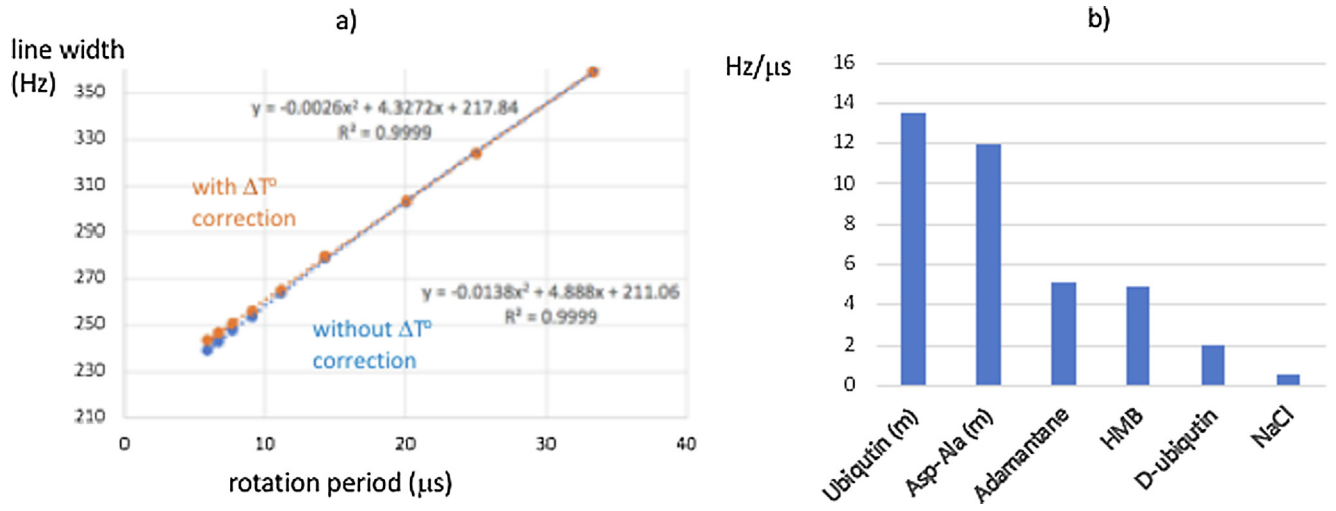

Fig. 4. (a) HMB linewidth as a function of rotation period. Temperature correction renders it linear with a coefficient of ≈4.3. (b) Linewidth/period coefficients for different spin systems. (m) is a median value of all resolved sites.

$$-A\int_0^{\tau}\cos(\omega t)dt = A\frac{\sin(\omega\tau)}{\omega}$$

A cumulative phase after time T in steps of duration τ is then

$$\Phi = -2\pi A\int_0^{\tau} cosdt\sqrt{\frac{T}{\tau}} = 2\pi A\frac{\sin(\omega\tau)}{\omega}\sqrt{\frac{T}{\tau}}$$

From this the linebroadening as $\Delta=1/\pi T_2'$ can in analogy to random walk above be evaluated as

$$\Delta \propto \frac{(A\sin(\omega\tau))^2}{\omega^2\tau}$$

If the correlation time, characterizing essentially a failure of spin phase to refocus after the rotor turn, is independent of rotation (angular) frequency ω, like in the case of mobility, a quadratic dependency can be expected. For a rigid lattice, the correlation time is related to spin-flips and, assuming their inverse probability with rotation speed

$$\tau \propto \frac{1}{\omega}$$

a principally linear line broadening on rotation period can be expected in accord with our experimental observations. The act of spin-flip constitutes also a decay in the number of coherent spins and adds to the line broadening, this process does not differ principally from the random tumbling in solvents. Slightly quadratic dependencies have been claimed in several papers on proton dense but wiggling bio-molecules which is well compatible with the mechanistic (hand-waving) interpretation above.

Apart improving the resolution, higher spinning rate may promote H-MAS in other practical ways. A particularly valuable feature, now transferable from the solution-NMR ammunition, is ^{1}H-^{15}N-^{1}H INEPT [12], a basic building block of a multidimensional NMR. The polarization transfer efficiency depends critically on T_2' of protons. For an optimally chosen interpulse delay value and J = 92 Hz, it will grow to over 20% for fully and 65% for a partially protonated structure at 170 kHz. Values are higher for ^{1}H–^{13}C bonds (J = 140), reaching also over 60% for fully protonated systems [13].

High speeds enable also direct detection of molecular mobilities by the virtue of *rf*-locking at the molecular dynamics timescale, observing $T_{1\rho}$. A critical feature here is adequate suppression of the dispersing residual dipolar interactions, which would otherways screen the resonant mobility contribution to the decay of magnetization. A molecular dynamics generated fluctuations in dipolar fields and chemical shift, matching the rate of spin nutation, accelerate the $T_{1\rho}$ relaxation at specific values of B_1 field. This method can be very informative and selective over a wide range of molecular motions as they are filtered out by the amplitude of spin-lock field. Due to small coils, MHz range nutation frequencies

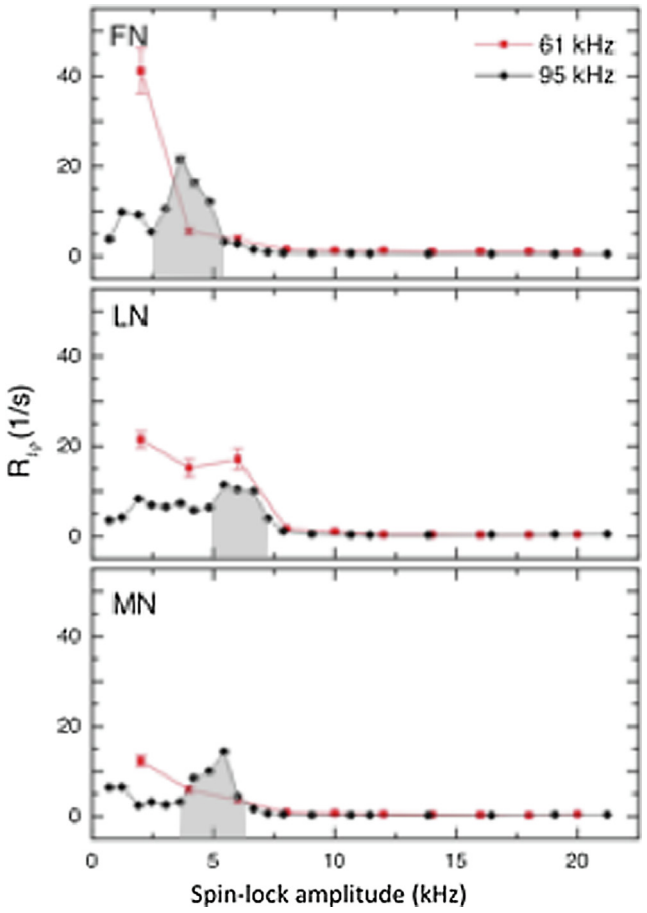

Fig. 5. ^{15}N relaxtion dispersion in tripeptide f-MLF. Each residue exhibits a different characteristic frequency of mobility, but only at a higher spinning rate.

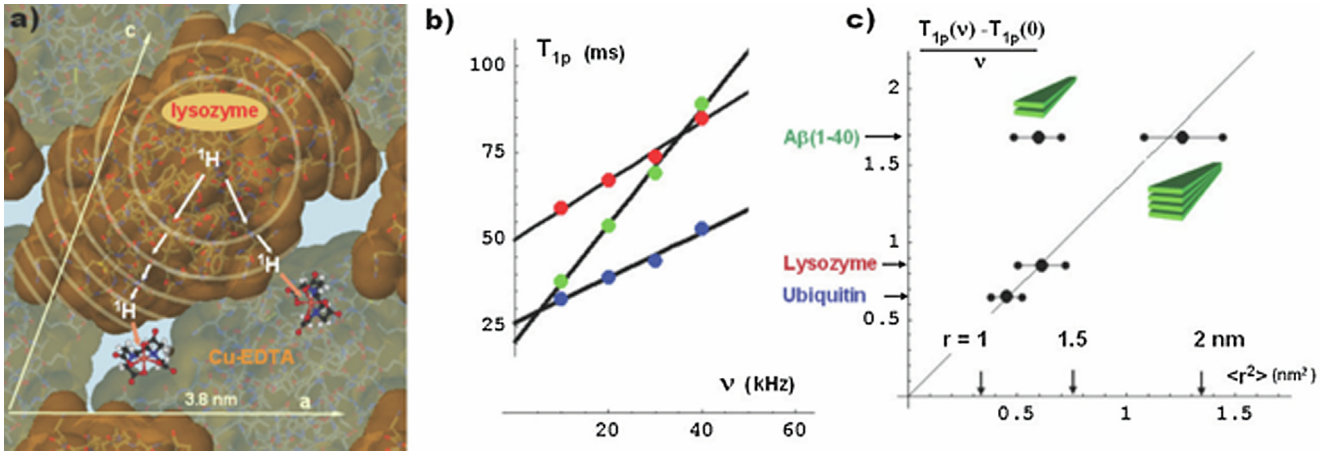

Fig. 6. Basic principles of the relaxation control. (a) Schematic presentation of relative size of proteins, Cu(II)EDTA and relaxation pathway in monoclinic lysozyme microcrystal. The protein molecules are drawn with a solvent accessible surface (PDB entry 6lyt), spin diffusion is illustrated by random walk distance after equal time intervals. (b) Experimental proton relaxation data of lysozyme (red), ubiquitin (blue) and amyloid fibril (green dots). (c) Correlation of the rate of relaxation time dependency on speed and the shape factor (error bars assume 10% variation in molecular dimensions). Two models of amyloid protofibril are considered. Radius r = 1 of a spherical protein is given for a reference. (For interpretation of the references to colour in this figure legend, the reader is referred to the web version of this article.)

can be achieved, providing mobility information at a μs scale. The destructive low speed effect is illustrated in Fig. 5.

There are numerous other applications which benefit from elevated speeds, like study of paramagnetic compounds or integer spin nuclei. The last is particularly interesting in the context of an inverse detection of ^{14}N overtone transitions [14].

Not only maximum spinning rate as such matters, the principal availability of wide range of spinning values may be a valuable experimental parameter. Line width variation rate (T_2') provides information on the local spin density (Fig. 3), this concept can be further elaborated in context of the spin diffusion and distance measurements.

One way to suppress other T_1 relaxation mechanisms is to amplify it by paramagnetic agents at a sufficiently high concentration. Then the measurement of spin T_1 relaxation diffusion from a distant paramagnetic layer as a function of the rotation speed can give quantitative information on shape factor $\langle r^2 \rangle = 1/(rx^{-2} + ry^{-2} + r_z^{-2})$ of the particle (Fig. 6) as

$$T_{1p}(\nu) \sim \kappa < r^2 > \nu_r + T_{1p}(0).$$

Remarkably, this method works without actual knowledge of the diffusion constant and does not require sieving of paramagnetic relaxation from other relaxation contributions. The analyses of experimental data of different protein samples shows indeed a linear dependency on the rotation speed ν_r (Fig. 6b). The rates of relaxation time change (Fig. 6c) correlate linearly with shape factors, calculated from the distances of periferial atoms (1.3, 1.1, 1.1) nm of ubiquitine and (2, 1.2, 1.2) nm of lysozyme respectively. Out of the two models of amyloid protofibril-single fold (1.5, 0.9, ∞) and back-to-back connected fold (1.5, 1.7, ∞), only the latter gives a similar correlation. This method can be for example used to profile cholesterol particles in blood.

The rotor speed can be changed not only parametrically, but in a real time too. The acceleration is in principle an inverse cube function of the diameter. Rotational resonances are among the most efficient known mechanisms of spin-recoupling [15], an adiabatic passage through a rotational resonance is very efficient in switching polarizations of both spins, for example from alpha-carbon to =CO and back to the next alpha along protein backbone. This feat has been demonstrated on the relayed coherence transfer and CP improvement with 1.8 mm rotors already [16], it can be used to study a spin diffusion and relaxation. Extrapolating data in Fig. 3 to increased drive pressures would give for the acceleration >10 kHz/ms.

H-MAS is bound to modulate considerably the progress and in particular bio-medical impact of NMR, maybe even divert it from a thermo-magnetic dead end. Higher magnetic fields require faster thermal motion for a line narrowing, whereas the logic of cell process research, arguably the most important NMR application area of all, is inherently interested in larger and with that slower molecular structures as they incarnate more valid functional models of life. Perdeuteration as a resolution saver is needed already for 50 kDa systems in solution. There is a notorius problem with any access to information on molecular activity at the cell membrane, despite this being a key wormhole to cellular/organ functionality in general and to any drug impact in particular. The H-MAS has already induced the shift of priorities for a new, yet to be delivered infrastructure: over half of 1.2 GHz instruments are conspired for the solid-state NMR. Apparently the physical dimensions of magnets and rotors correlate inversely. H-MAS is comin' to town [17].

Acknowledgement

This essay has been supported by Estonian research project PUT 1534 and ideas, technical help and discussions of J. Lewandowski, G. Otting, B. Meier, M.L. Org and A. Oss.

References

[1] A. Samoson et al., 100+ kHz MAS NMR, EUROMAR 2012, in: Magnetic Resonance Conference; 1–5 July: University College. Dublin, Ireland, 2012, p. 247.
[2] V. Agarwal et al., De novo 3D structure determination from sub- milligram protein samples by solid-state 100 kHz MAS NMR spectroscopy, Angew. Chem. Int. Ed. 53 (2014) 12253–12256.
[3] J.M. Lamley, D. Iuga, C. Öster, H.-J. Sass, M. Rogowski, A. Oss, J. Past, A. Reinhold, S. Grzesiek, A. Samoson, J.R. Lewandowski, Solid-state NMR of a protein in a precipitated complex with a full-length antibody, J. Am. Chem. Soc. 136 (48) (2014) 16800–16806, https://doi.org/10.1021/ja5069992.
[4] Susanne Penzel, Andres Oss, Mai-Liis Org, Ago Samoson, Anja Böckmann, Matthias Ernst, Beat H. Meier, Spinning faster: protein NMR at MAS frequencies up to 126 kHz, J. Biomol. NMR 73 (2019) 19–29.
[5] Y.-L. Lin et al., Preparation of fibril nuclei of beta-amyloid peptides in reverse micelles, Chem. Commun. 54 (2018) 10459–10462.
[6] A. Samoson et al., Fast magic-angle spinning: implications, in: Encyclopedia of Magnetic Resonance, John Wiley & Sons, Ltd, 2010, https://doi.org/10.1002/9780470034590.emrstm1017.

[7] N.P. Wickramasinghe, S. Parthasarathy, C.R. Jones et al., Nanomole-scale protein solid-state NMR by breaking intrinsic 1H T1 boundaries, Nat. Meth. 6 (2009) 215–218. Carl Öster, Simone Kosol, Christoph Hartlmüller, Jonathan M. Lamley, Dinu Iuga, Andres Oss, Mai-Liis Org, Kalju Vanatalu, Ago Samoson, Tobias Madl, Józef R. Lewandowski, Characterization of protein-protein interfaces in large complexes by solid-state NMR solvent paramagnetic relaxation enhancements, J. Am. Chem. Soc. 139(35) (2017) 12165−12174. doi:10.1021/jacs.7b03875.

[8] Y. Ishii, R. Tycko, Sensitivity enhancement in solid state 15N NMR by indirect detection with high-speed magic angle spinning, J. Magn. Reson. 142 (2000) 199.

[9] A.P.M. Kentgens, J. Bart, P.J.M. van Bentum, A. Brinkmann, E.R.H. van Eck, J.G.E. Gardeniers, J.W.G. Janssen, P. Knijn, S. Vasa, M.H.W. Verkuijlen, High-resolution liquid- and solid-state nuclear magnetic resonance of nanoliter sample volumes using microcoil detectors, J. Chem. Phys. 128 (2008) 052202, https://doi.org/10.1063/1.2833560.

[10] U. Sternberg et al., 1H line width dependence on MAS speed in solid state NMR—comparison of experiment and simulation, J. Magn. Reson. 291 (2018) 32–39.

[11] Vadim E. Zorin, Steven P. Brown, Paul Hodgkinson, Origins of linewidth in H 1 magic-angle spinning NMR, J. Chem. Phys. 125 (2006) 144508, https://doi.org/10.1063/1.2357602.

[12] Gareth A. Morris, Ray Freeman, Enhancement of nuclear magnetic resonance signals by polarization transfer, J. Am. Chem. Soc. 101 (3) (1979) 760–762, https://doi.org/10.1021/ja00497a058.

[13] S. Penzel, A.A. Smith, V. Agarwal, A. Hunkeler, M.-L. Org, A. Samoson, A. Bökmann, M. Ernst, B.H. Meier, Protein resonance assignment at MAS frequencies approaching 100 kHz: a quantitative comparison of J-coupling and dipolarcoupling-based transfer methods, J. Biomol. NMR 63 (2) (2015) 165–186, https://doi.org/10.1007/s10858-015-9975-.

[14] S. Cavadini, S. Antonijevic, A. Lupulsescu, G. Bodenhausen, J. Magn. Reson. 182 (2006) 168.

[15] D.P. Raleigh, M.H. Levitt, R.G. Griffin, Rotational resonance in solid state NMR, Chem. Phys. Lett. 146 (1–2) (1988) 71–76.

[16] A. Samoson, T. Tuherm, J. Past, Rotation sweep NMR, Chem. Phys. Lett. 365 (2002) 292–299.

[17] J.F. Coots, H. Gillespie, Eddie Cantor's Radio Show, November 1934.